Molecular deformation processes in an ethylene copolymer under tensile drawing: static and dynamic study by means of Fourier transform infra-red spectroscopy

J. Dupuis* and P. Legrand
Laboratoire de Spectrochimie Infrarouge et Raman, UP CNRS 2641, Université de Lille I, 59655 Villeneuve d'Ascq Cedex, France

and R. Seguelat and F. Rietsch
Laboratoire de Structure et Propriétés de l'Etat Solide, UA CNRS 234, Université de Lille I, 59655 Villeneuve d'Ascq Cedex, France
(Received 19 June 1987; revised 30 September 1987; accepted 28 October 1987)

Static and dynamic orientation measurements have been performed by means of Fourier transform infra-red spectroscopy in order to characterize the uniaxial drawing behaviour of an ethylene/1-butene copolymer. The orientational evolution of the crystalline bands in the static study has shown that the plastic deformation probably proceeds by untwisting of the original lamellar ribbons, before the onset of the fibrillar transformation. The assignment of some infra-red-active amorphous conformations with various kinds of chains has been discussed by considering their orientational behaviour. The dynamic study has revealed relaxation processes of the amorphous chains together with strain-induced crystallization, in a range of time up to a few tens of milliseconds after neck completion.

(Keywords: ethylene copolymer; tensile drawing; infra-red spectroscopy; chain orientation; relaxation; crystallization)

INTRODUCTION

Infra-red spectroscopy is a powerful tool to investigate chemical and physical changes in polymers on a molecular scale[1,2]. Besides, polymers exhibit i.r. dichroism, which is particularly well suited for providing an insight into the molecular processes of deformation[3]. Knowledge of these processes is indeed of great interest when one is concerned with the improvement of mechanical properties of polymeric materials. In this connection, i.r. spectroscopy would be particularly appropriate for studying the drawing behaviour of linear low-density polyethylene (LLDPE), which can provide high-strength fibres with good creep resistance[4-6].

Early static i.r. studies devoted to the necking of polyethylene (PE) have shown that the crystalline phase deforms according to shear processes that progressively bring the chain axis parallel to the drawing direction, in order to promote chain unfolding[7,8]. Glenz and Peterlin have reported a series of papers[9-11] demonstrating that the amount of *trans* conformations in the amorphous chains of drawn polyethylene grows at the expense of the *gauche* conformations, with a concomitant transformation of folding loops into intercrystalline tie molecules as the draw ratio increases. McRae and Maddams[12,13] have further tried to relate the orientational behaviour of some crystalline and amorphous bands to the mechanical properties of oriented blown films or drawn samples, especially the stress crack resistance. A correlation between the overall amorphous chain orientation and the tensile strength of polyethylene fibres has also been successfully attempted by Marikhin *et al.*[14]

Dynamic studies have been carried out more recently following the development of Fourier transform infra-red (*FT*i.r.) spectroscopy. Holland-Moritz *et al.*[15,16] and Siesler[3,17] have reported transient regime studies of the plastic deformation in high-density polyethylene, which corroborate the previous conclusions from static studies as concerns the crystal orientation during the build-up of the neck. Also, the gradual and partial transformation of the crystalline phase from the orthorhombic form to the monoclinic form has been particularly well emphasized by Siesler[3,17] as a function of strain, in a more systematic and conspicuous way than already revealed by X-ray measurements[18,19]. However, only the most intense bands ascribed to the crystalline phase have been investigated using low drawing rates of about $10^{-2}\,s^{-1}$, because of time constraints imposed by the recording of the *FT*i.r. spectra.

In order to investigate the effect of high-speed stretching, we have contrived a steady-state drawing device (i.e. dynamic drawing at constant draw ratio), which allows us to study amorphous bands without any constraint on the recording times. This equipment is based on an industrial drawing bench, which involves the pulling of a continuous yarn or strip between two sets of feed rollers and draw rollers, the ratio of the draw-roller speed to the feed-roller speed determining the draw ratio. Thus, we have been able to obtain insight into the dynamic behaviour of the amorphous chains of an LLDPE during the course of drawing, for linear speeds up to $50\,m\,min^{-1}$.

* This work is a part of J. Dupuis' Doctoral Thesis
† To whom correspondence should be addressed

0032-3861/88/040626-08$03.00

EXPERIMENTAL

Sample preparation

The polymer studied[4,5] is an ethylene/1-butene copolymer supplied by CdF Chimie. The number- and weight-average molecular weights are $M_n = 4.6 \times 10^4$ and $M_w = 1.6 \times 10^5$. The nominal density is $\rho = 0.930\ g\ cm^{-3}$. The samples used for the drawing experiments were in the form of strips cut from films produced by the tubular blowing method under low-stress conditions. The strips were cut parallel to the extrusion direction. The static study was performed with three kinds of films of 50, 200 and 650 μm thickness for the characterization of the sharp, medium and weak i.r. bands, respectively, in accord with the Beer–Lambert law. For the dynamic study, only the 200 μm thick samples were used, the length of which was about 400 m.

Drawing procedure

The specimens investigated in the static study were drawn at 80 and 110°C by means of an Instron tensile testing machine equipped with an environmental chamber. The cross-head speed was fixed at 50 mm min^{-1} for samples about 50 mm long and 15 mm wide. The hot-drawn samples were subsequently cooled to room temperature under constant length before unloading.

The dynamic study was carried out on a drawing bench whose design is sketched in *Figure 1*. Necking usually occurred close to the end of the oven, which could be moved between the two sets of rollers in order to select the location of the i.r. beam along the sample. The drawing temperature $T_d = 110°$ was controlled by means of an i.r. camera focused on the sample at the oven exit. The feed-roller speed V_f was kept constant at 5 m min^{-1} while the draw-roller speed V_d could vary between 5 and 50 m min^{-1}. The draw ratio was defined as V_d/V_f.

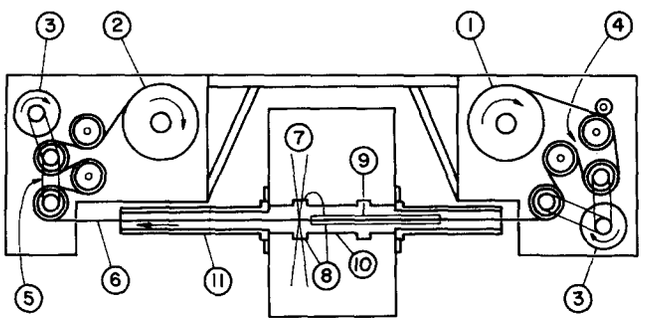

Figure 1 Drawing bench for dynamic infra-red measurements: (1) feed bobbin, (2) take-up bobbin, (3) driving engines, (4) feed-roller set, (5) draw-roller set, (6) sample, (7) infra-red beam, (8) KRS-5 windows, (9) moving oven, (10) insulated sample compartment, (11) glass tube

Infra-red measurements

The instrument was a Bruker IFS 113V Fourier transform infra-red spectrometer operated under vacuum and provided with a mercury–cadmium–tellurium detector. It was also fitted with a germanium-wire-grid polarizer, which allowed dichroic measurements. The width of the i.r. beam focused on the sample was about 4 mm.

The static i.r. study was carried out at room temperature using unloaded samples previously allowed to relax for several days after drawing. On the other hand, the i.r. measurements relating to the dynamic study were performed during the course of drawing at 110°C. In this latter case, the insulated vacuumless sample compartment in which the oven can be moved longitudinally was equipped with temperature-resistant and non-hygroscopic windows made of KRS-5 thallium bromoiodide. More details about the dynamic i.r. experiments and related operations will be published elsewhere[20].

The i.r. spectra (having a 2 cm^{-1} resolution) consisted of 64 scans recorded over an acquisition period of 48 s. The overlapping bands were resolved by means of a computer-assisted fitting method (Bruker Bandsim Program) involving an adjustable combination of Gaussian and Lorentzian band profiles. The assignment of the characteristic i.r. bands of polyethylene is detailed in *Table 1*, after Krimm[21] and Snyder[22].

The dichroic ratios have been determined from polarized i.r. measurements according to the relation:

$$D = A_{\parallel}/A_{\perp}$$

where $A_{\parallel}$ and $A_{\perp}$ are the absorbances measured with the polarized radiation parallel and perpendicular to the draw direction, respectively. The orientation functions have been computed consecutively from the following equation:

$$f = \frac{(D-1)/(D+2)}{\frac{1}{2}(3\cos^2\beta - 1)}$$

Table 1 Assignment of the selected i.r. bands of polyethylene[a]

Wavenumber (cm^{-1})	Intensity[b]	Phase[c]	Transition moment	Assignment
720	S	C (+A)	$\parallel b$	Out-of-phase CH_2 rocking mode
730	S	C	$\parallel a$	In-phase CH_2 rocking mode
909	W	A	$\perp$ chain axis	CH_2 wagging mode in the vinyl end groups
1080	W	A	$\perp$ chain axis	Skeletal C–C stretching mode in *g* and *t* conformations
1303	M	A	$\parallel$ chain axis	CH_2 wagging mode in *gtg* and *gtg'* conformations
1352	M	A	$\parallel$ chain axis	CH_2 wagging mode in *gg* conformations
1368	M	A	$\parallel$ chain axis	CH_2 wagging mode in *gtg* and *gtg'* conformations
1894	W	C	$\perp c$	Combination between the 1168 cm^{-1} Raman-active band and the 720 and 730 cm^{-1} i.r. bands
2016	W	C (+A)	$\parallel$ chain axis	Combination between the 1295 cm^{-1} Raman fundamental and the 720 and 730 cm^{-1} i.r. bands plus combination between the 1303 and 720 i.r. bands

[a] According to refs. 21 and 22
[b] S, strong; M, medium; W, weak
[c] C, crystalline phase; A, amorphous phase

β being the angle between the chain axis (or a crystal axis) and the direction of the transition moment.

Unpolarized i.r. measurements have been performed to determine the reduced structure factor A'_ν of various bands of wavenumber ν, according to the relation:

$$A'_\nu = A_\nu / A_{909}$$

where A_ν and A_{909} are the absorbances of the ν and 909 cm^{-1} bands, respectively. The reduced structure factor allows comparisons to be made between various i.r. bands, irrespective of the changes in crystallinity and thickness of the samples[9,10].

STATIC INFRA-RED STUDY OF THE DRAWING

Crystal orientation

The 720, 730 and 1894 cm^{-1} bands have been analysed in order to characterize the orientation of the crystal unit cell as a function of the deformation, neglecting the small amorphous contribution to the 720 cm^{-1} band. *Figure 2* shows the variation of the orientation functions f_a, f_b and f_c of the crystallographic axes with the draw ratio λ, for two drawing temperatures $T_d = 80°C$ and 110°C. The c axis, or chain axis in the crystal, orients gradually towards the draw direction. In parallel, the a and b axes orient perpendicular to the draw direction but, for $T_d = 80°C$, the orientation of the b axis is much slower than that of the a axis. This trend could have been regarded as an artifact due to the small amorphous contribution to the 720 cm^{-1} band if not confirmed by the X-ray data reported in *Figure 3*, according to a previous work dealing with the same material[5]. Moreover, a similar behaviour had already been reported for high- and low-density polyethylene, from X-ray[23] as well as i.r. dichroic measurements[17,24].

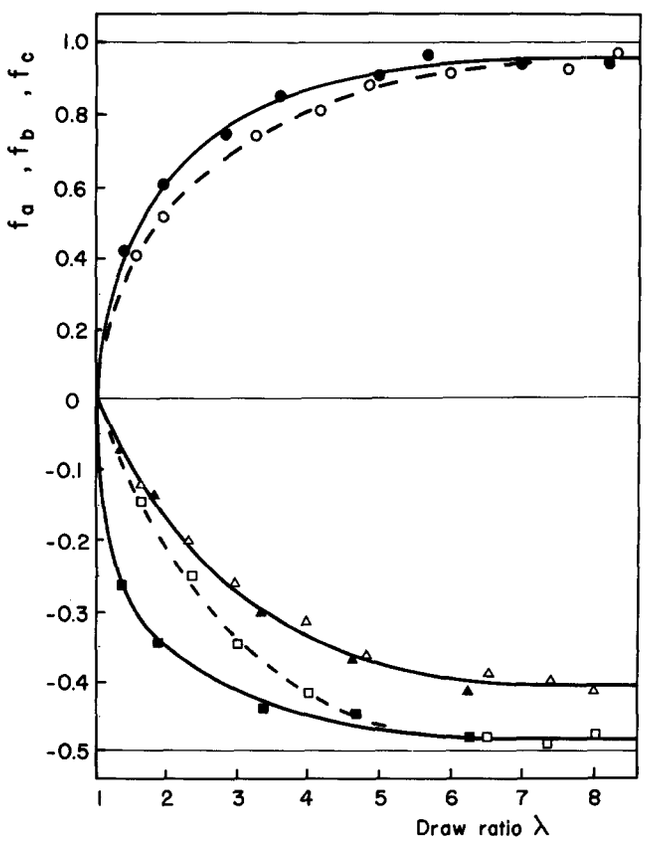

Figure 2 Orientation functions of the crystal axes from dichroic infra-red measurements *versus* static draw ratio: (■, □) a axis, (▲, △) b axis, (●, ○) c axis; full symbols and full curves refer to $T_d = 80°C$; open symbols and broken curves refer to $T_d = 110°C$

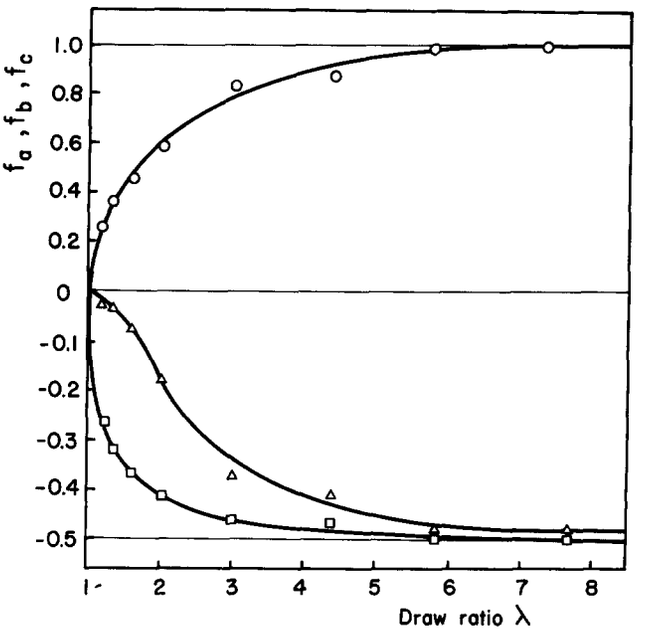

Figure 3 Orientation functions of the crystal axes from X-ray measurements *versus* static draw ratio: (□) a axis, (△) b axis, (○) c axis; $T_d = 80°C$

In a series of rheo-optical studies of polyethylene in the elastic range of strains, Kawai *et al.*[25-27] suggested that the orientation of the crystal about the b axis is related to the untwisting of the lamellar ribbons, whereas the orientation about the a axis arises from rotation of the lamellae as a whole or as mosaic blocks, the first process operating predominantly in equatorial regions. This result is in agreement with the earlier optical microscopic study of the deformation of thin PE films reported by Hay and Keller[28]. These authors have further pointed out that the rotation of the crystal axes occurs more readily about the b axis than about the a axis. Both processes of crystal axis orientation are sketched in *Figure 4*, which represents two intermeshed portions of neighbouring twisted lamellae in a PE spherulite. The higher rate of the a axis orientation observed for $T_d = 80°C$ (*Figures 2* and *3*) gives an indication that untwisting is an easier deformation process than tilting of the lamellae as a whole. Indeed, the smaller transverse dimension of the lamellar ribbons makes them more prone to untwist around the b axis during the former stage of the deformation whose basic trend is to bring the chain axis into the best orientation for slippage of the crystal blocks that promotes the fibrillar transformation[29].

For the drawing temperature $T_d = 110°C$, the orientation of the a axis takes place at a lower rate than for $T_d = 80°C$ (*Figure 2*), the orientation of the b axis following the same trend for both temperatures. It is likely that, owing to the higher ductility of the crystalline phase at $T_d = 110°C$, the slippage of the crystal blocks could proceed more gradually before the chains reach the appropriate orientation. This interpretation is supported by the comparative analysis by Peterlin and Meinel[30] of hot and cold drawing in the small-strain range.

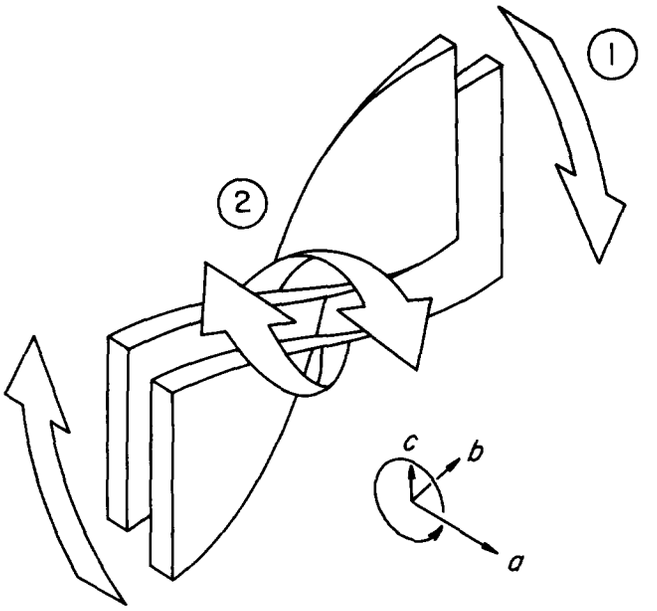

Figure 4 Orientation processes of the crystal axes in twisted lamellar ribbons of polyethylene: (1) lamellar tilting for *b* axis orientation; (2) lamellar untwisting for *a* axis orientation

Amorphous chain orientation

The orientation functions of the five bands characteristic of the purely amorphous chain conformation are shown in *Figure 5* as a function of draw ratio. Also shown in *Figure 5*, for the sake of comparison, is the 2016 cm^{-1} band, which contains both amorphous and crystalline contributions. The general trend, consisting of a gradual increase and saturation of the orientation functions, is similar to the observation reported in previous i.r. studies concerned with the drawing behaviour of high- and low-density PE[9,10,24,31,32]. The overall amorphous orientation (1080 cm^{-1} band) levels off at $f_{1080} \simeq 0.3$, i.e. well below the *c* axis crystal orientation (*Figure 2*). On the other hand, the 909 cm^{-1} band ascribed to the vinyl end groups exhibits a significantly higher limiting value of the orientation function, $f_{909} \simeq 0.45$, indicating that these groups are very sensitive to the crystal orientation, as previously suggested by Miller *et al.*[33] It is suspected that this phenomenon could be due to either a partial accommodation of the vinyl groups within the crystal or a retention effect of the crystal orientation by the shorter chain cilia emerging normal to the crystal surface. This point will be developed further in the 'Dynamic study' section.

The 1303, 1352 and 1368 cm^{-1} bands characteristic of *gauche*-rich conformations display lower orientation than the previous ones. This is quite logical since it is well known that the *trans* conformations themselves develop at the expense of the *gauche* ones as a function of draw ratio[9,32], indicating that the remaining *gauche* conformations must more probably be located in the less strained chains. What is quite amazing, however, is the contrast of orientational behaviour between the 1368 and 1303 cm^{-1} bands. Indeed, the limiting orientation of the former band is about five times greater than that of the latter, although the two bands have usually been associated with both *gtg* and *gtg'* conformation sequences[9,24,33]. In fact, Snyder[22] has pointed out that the origin of the 1368 cm^{-1} band lies more probably in the sole *gtg* conformation sequences, for reasons of symmetry of the CH_2 wagging mode with respect to the central *trans* conformation. Owing to this distinctive attribution of the two bands, an interpretation can be proposed for their peculiar orientational behaviour. The schematic conformational views of *Figure 6* show conspicuously that a *gtg'* sequence is much more 'open' than a *gtg* one (the end-to-end distance is greater for the *gtg'* conformation than for the *gtg* one). Consequently, for a given strain, the *gtg'* sequences are likely to be less oriented than the *gtg* sequences. On the other hand, the reduced structure factors of the 1368 and 1303 cm^{-1} bands shown in *Figure 7* indicate that both conformations follow roughly the same receding trend with increasing draw ratio, as a result of *gauche–trans* isomerization. The opposition between these two features suggests that *gtg'* and *gtg* conformation sequences are mainly located within chains of different deformation behaviours, which seems in contradiction with McRae and Maddams' proposal[13] that both conformations belong to folding loops.

The 1352 cm^{-1} band is associated with the thermodynamically unfavourable *gg* conformations,

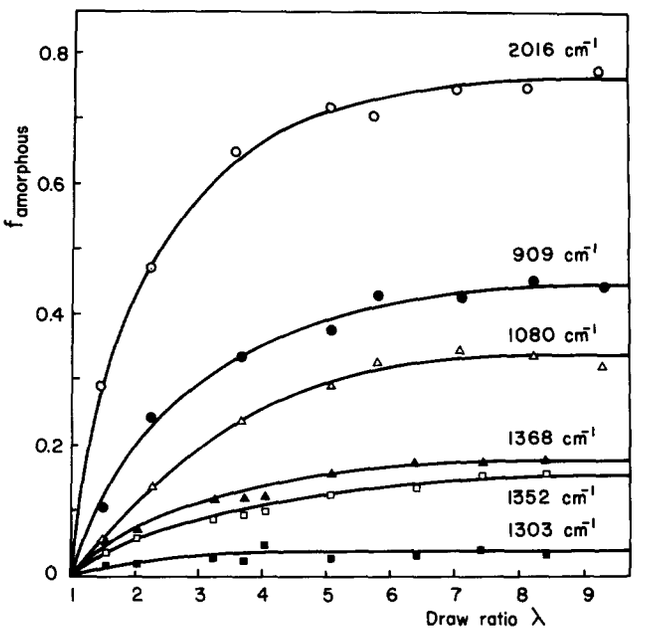

Figure 5 Orientation functions of amorphous chain conformations *versus* static draw ratio; $T_d = 80°C$ (the infra-red band wavenumbers are given—see *Table 1* for the assignments)

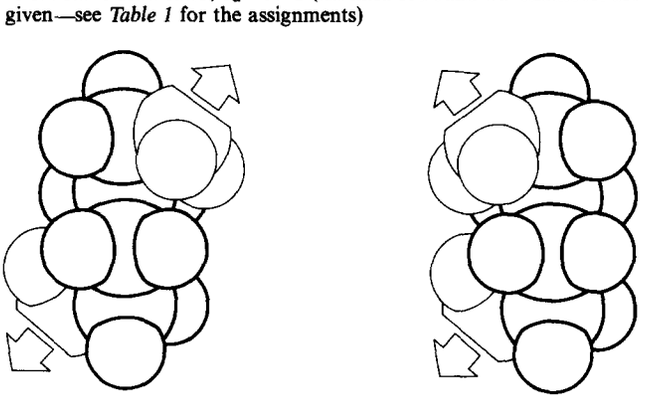

gtg' conformation *gtg* conformation

Figure 6 Schematic representation of *gtg* and *gtg'* conformation sequences in a polyethylene chain (the arrows indicate chain prolongation)

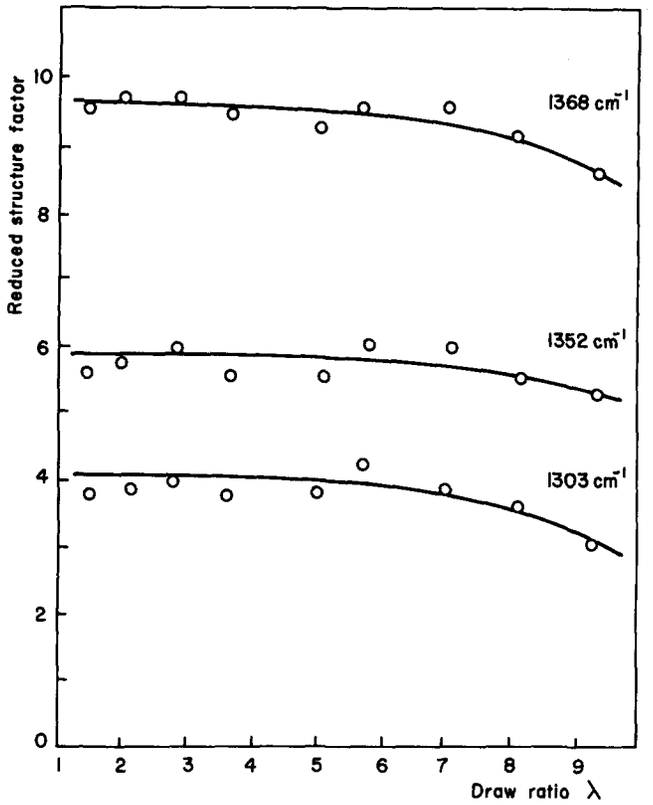

Figure 7 Reduced structure factor of the 1303, 1352 and 1368 cm^{-1} amorphous bands as a function of static draw ratio; $T_d = 80°C$

which more probably belong to chain segments in a bent state, such as sharp folds. Indeed, previous conformational[34,35] and spectroscopic[36] studies of chain folding in PE have shown that sharp folds should accommodate a high concentration of *gg* conformation pairs. Any disordered chain segment is also expected to contain some *gg* conformation pairs. However, *Figure 7* shows that the 1352 cm^{-1} band is not very sensitive to *gauche–trans* isomerization, indicating that it is concerned with constrained *gg* pairs rather than with purely statistical ones. Hence, the orientation of the *gg* pairs can be ascribed chiefly to the plastic shear of the crystal blocks, which leads to an elongation of the folds in the direction of the shear[37,38].

The 2016 cm^{-1} band displays a much stronger orientational behaviour than the previous amorphous bands (*Figure 5*), as a logical result of the crystalline contribution. It is, however, worth noting that the limiting value of the orientation function, $f_{2016} \simeq 0.75$, is close to the value of the mean orientation function, $\bar{f} \simeq 0.72$, which can be estimated from the limiting orientation functions of the crystal *c* axis (1894 cm^{-1} band in *Figure 2*) and the overall amorphous phase (1080 cm^{-1} band in *Figure 5*) according to the relation:

$$\bar{f} = f_{1894}\alpha_c^w + f_{1080}(1-\alpha_c^w)$$

in which the crystal weight fraction is set as $\alpha_c^w = 0.63$ for $\lambda = 9$ (ref. 5). This remark suggests that the amorphous contribution to the 2016 cm^{-1} band may arise from both *trans* and *gauche* conformations (*Table 1*) rather than from *trans* sequences only as proposed by Read and Stein[24].

DYNAMIC INFRA-RED STUDY OF THE DRAWING

The dynamic i.r. analysis has been carried out for two points of observation during the course of the drawing process. These points are located at the end of the neck and 2 cm downstream on the samples, as shown in the schematic drawing of *Figure 8*. The neck being perfectly stable, the phenomenological situation for each point of observation can be considered as a steady state. Samples 200 μm thick were only available in the form of very long strips cut from tubular blown films, so none of the purely crystalline bands could be investigated.

Purely amorphous 1303, 1352 and 1368 cm^{-1} bands

The orientation functions of the 1303, 1352 and 1368 cm^{-1} bands are shown in *Figure 9* for the two points of observation, in a range of draw ratios beyond the neck, i.e. $5.5 < \lambda < 9$. Every band displays a very small increase of orientation with draw ratio akin to that observed in the static study (*Figure 5*), in the same range of strain. On the other hand, a large drop in the orientation functions appears between the two points of observation, the values at point 2 being close to those reported in the static study (*Figure 5*). This is evidence that the deformation mechanism accompanying neck formation, namely the fragmentation of the crystalline lamellae into blocks that realign themselves to build up microfibrils[29], involves an excessive transient orientation of the amorphous chains, which quickly relieves their overstressing after neck completion. The spectra of *Figure 10* show that the absorbance of the 1352 and 1368 cm^{-1} bands grows in the meantime between the two measurements at point 1 and point 2, indicating a recovery of the *gauche* conformations, which reinforces the concept of a relaxation process. Moreover, the progressive martensitic-like transformation of the crystalline phase reported by Siesler[17] along with neck formation, and its partial recovery after neck completion, provide further support for the overstressing effect on the crystals and the amorphous chains too, owing to the fact that these last ones carry the load onto the crystals.

It is worth mentioning that our conclusion about amorphous chain relaxation is in agreement with the theoretical approach of strained polymer dynamics. According to this theory[39], the entropic restoring forces allow a chain in the melt to be relieved from a state of strain within a characteristic equilibration time τ_e, which is related to the overall renewal time τ_r by the following equation:

$$\tau_r = 3(M_o/M_e)\tau_e$$

where M_o and M_e are the overall molecular weight of the chain and the molecular weight between entanglements, respectively. Yoon and Flory[40] have estimated the time

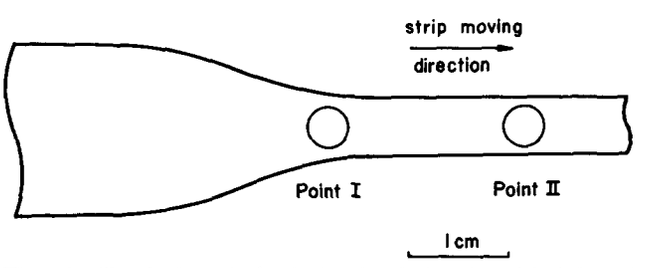

Figure 8 Sketch of a necked strip showing the location of the infra-red beam for the two points of observation in the dynamic study

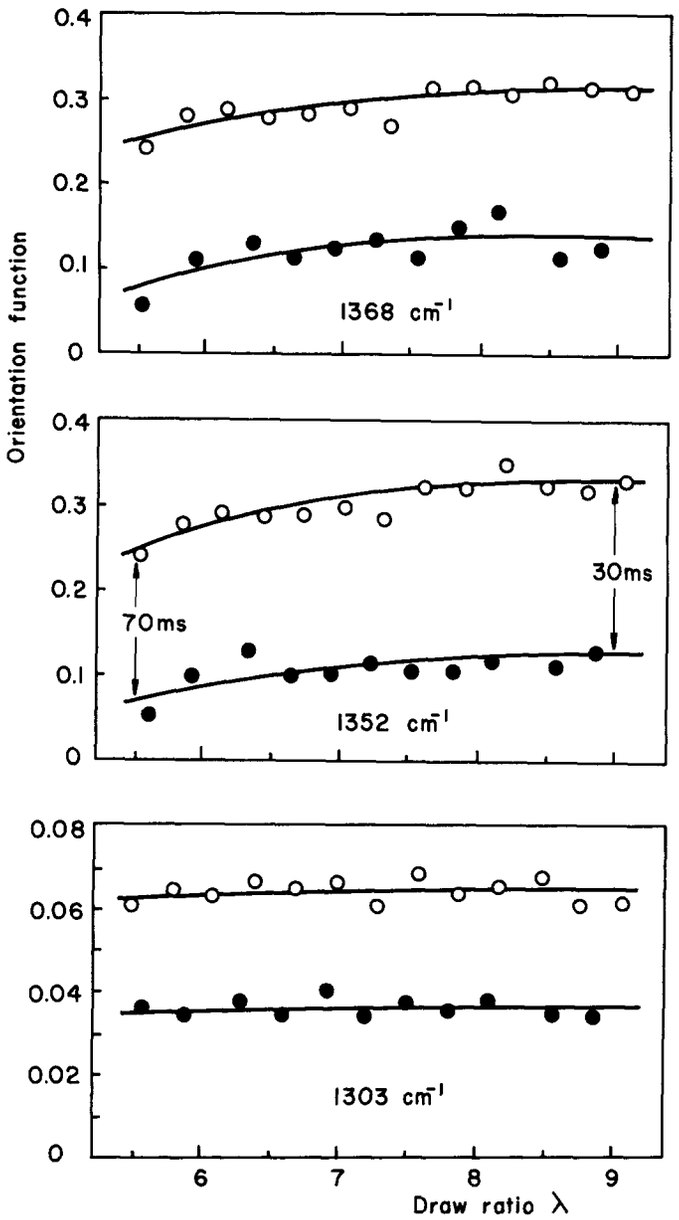

Figure 9 Orientation functions of amorphous chain conformations *versus* draw ratio in the dynamic regime at $T_d = 110°C$: (○) point 1 and (●) point 2 of observation according to *Figure 8* (the infra-red band wavenumbers are given—see *Table 1* for the assignments)

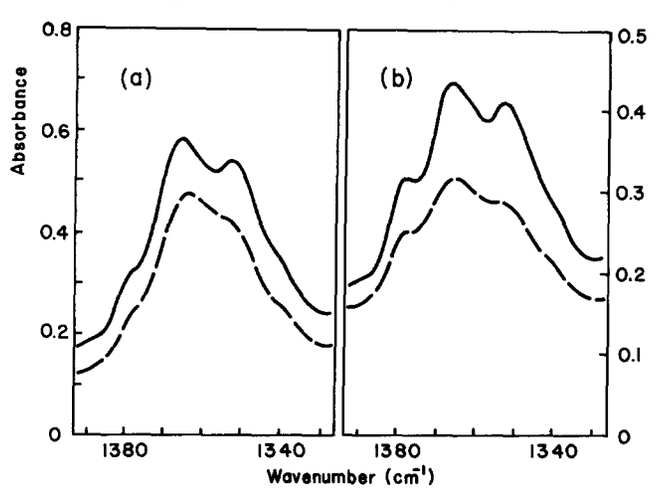

Figure 10 Infra-red spectra recorded in the dynamic regime at $T_d = 110°C$ for a draw ratio $\lambda = 5.8$: infra-red beam polarized (a) parallel and (b) perpendicular to the draw direction. The broken curve and the full curve refer respectively to observation points 1 and 2 according to *Figure 8*

required for a PE chain of molecular weight $M = 10^5$ to diffuse over its whole length to be about 1 s, at $T = 120°C$. So, assuming that this is τ_r and taking $M_e \simeq 2000$ for PE in the melt[41], we can assess τ_e to be less than 10 ms. On the other hand, considering the distance between the two points of observation in our study and the drawing velocity of the strips, we can infer that the intervals between the two experiments along the samples vary from 30 to 70 ms, depending on the draw ratio (*Figure 9*). Accordingly, enough time is afforded for the relaxation of the amorphous chains to occur.

A remark must be made concerning the 1352 cm^{-1} band preferentially ascribed to sharp folds. Indeed, the relaxation of these amorphous molecules, which bridge the glide planes, implies that a reverse shear relaxation of the sheared crystal blocks occurs concomitantly.

Crystal-sensitive 909 and 2016 cm^{-1} bands

The orientation function of the 909 cm^{-1} band associated with the vinyl end groups is reported in *Figure 11* as a function of the draw ratio beyond the neck. This figure shows that the 909 cm^{-1} band exhibits an orientational behaviour opposite to that of the previous amorphous bands, the orientation function increasing from point 1 to point 2 of observation. This improvement of the vinyl end group orientation after neck completion can be related to the phenomenon of strain-induced crystallization, which is well known to take place beyond the neck for high- and low-density polyethylene[5,9]. Indeed, we have pointed out in the previous section that the chain end orientation is strongly sensitive to the crystal orientation. So, the strain-induced crystallization of some originally amorphous chains together with chains that have been pulled out of the crystal blocks after fragmentation of the lamellar ribbons is expected to enforce a better alignment of the vinyl groups parallel to the draw direction, in the post-yield region. In this connection, it must be emphasized that the rate of chain deposition on a crystal surface is $g \simeq 10^2\ ms^{-1}$ for the crystallization of a PE having a molecular weight $M = 10^5$, in a range of temperature about $T = 120°C$[40,42]. Thereby, one can estimate the time required for the crystallization of an entire chain to be about 10 ms. Such an interval is short enough to allow crystallization of the whole chain between the two measurements carried out at points 1 and 2. This conclusion applies *a fortiori* to portions of chains under strain and provides support for

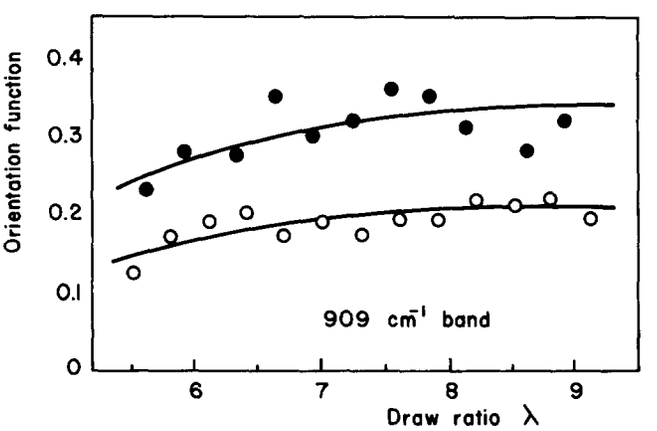

Figure 11 Orientation function of the vinyl end groups *versus* draw ratio in the dynamic regime at $T_d = 110°C$: (○) point 1 and (●) point 2 of observation according to *Figure 8*

our interpretation of the incidence of strain-induced crystallization on the orientational behaviour of the chain ends.

The limiting value of the orientation function of the vinyl groups at observation point 2 (*Figure 11*) is lower than that reported in the previous static study (*Figure 5*), at room temperature. This must be due to the partial melting of the copolymer at the drawing temperature $T_d = 110°C$. The d.s.c. trace of *Figure 12* indeed shows that the crystallinity at 110°C of a fibre having a draw ratio $\lambda = 8.3$ is about 75% of the room-temperature crystallinity. Therefore, the vinyl end groups are liable to undergo a post-drawing increase of orientation during cooling of the samples, owing to the oriented crystallization of the low-melting fraction according to an epitaxial growth process over the already oriented fibrils.

Figure 13 displays the orientational behaviour of the 2016 cm^{-1} band. The relaxation process that occurs between the points 1 and 2 of observation is similar to that reported in *Figure 9* for the 1303, 1352 and 1368 cm^{-1} bands. However, the magnitude of the relaxation is much less important for the 2016 cm^{-1} band than for the three other amorphous bands. This suggests that the crystalline orientation is affected much less than the amorphous one by the chain relaxation that occurs in the post-yield region. The limiting value of the orientation function is lower than the limiting value observed in the static study (*Figure 5*). This is certainly due to the partial melting of the copolymers at the drawing temperature of 110°C, as previously discussed in the case of the 909 cm^{-1} band. As a matter of fact, an increase in the weight fraction of the amorphous phase, which has a weaker orientation than the crystal, must lead to a lower overall orientation at 110°C, as compared to room temperature.

A theoretical determination of the limiting orientation functions of the 909 and 2016 cm^{-1} bands at 110°C would be worth performing. Unfortunately, neither the crystal orientation function nor the precise degree of crystallinity can be obtained from the i.r. measurements carried out in the dynamic study because of the unsuitable sample thickness for investigation of purely crystalline bands.

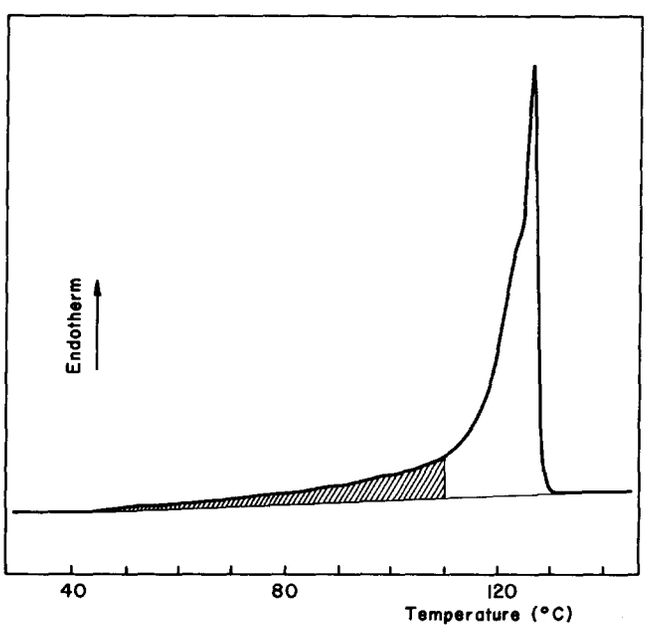

Figure 12 D.s.c. melting curve for a fibre drawn at $T_d = 110°C$ and having a draw ratio $\lambda = 8.6$ (see ref. 5 for the recording conditions)

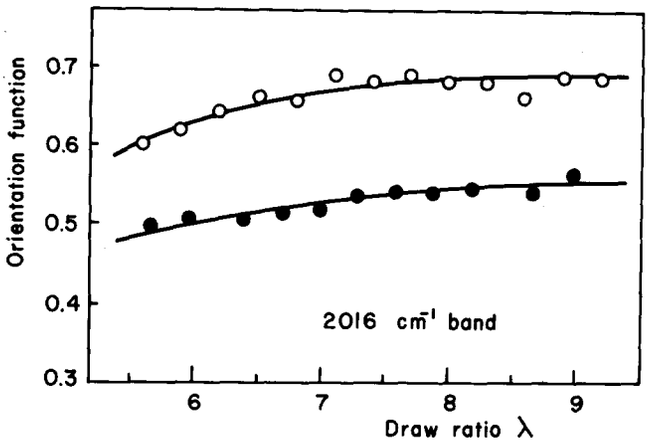

Figure 13 Orientation function of the overall crystalline and amorphous chain conformations *versus* draw ratio in the dynamic regime at $T_d = 110°C$: (○) point 1 and (●) point 2 of observation according to *Figure 8*

CONCLUSIONS

New information about the deformation mechanisms involved on the molecular scale during hot drawing of LLDPE has been obtained from an i.r. spectroscopic study. The investigations performed in static mode, i.e. after the completion of drawing, the sample being unloaded, have shown that the crystalline phase undergoes a quick orientation of the *c* axis towards the draw direction, the basic process of which seems to be the untwisting of the lamellar ribbons. The amorphous phase orients more gradually and to a much lower extent than the crystal, as a function of the draw ratio. We have discussed the specific assignment of some i.r.-active amorphous conformations with different types of chains according to their orientational trends with drawing. The *gtg'* and *gtg* conformations should preferentially belong to chains having distinct deformation behaviours. It is also suggested that the *gg* conformation pairs are concentrated in sharp folds, which make them sensitive to the plastic shear of the crystal blocks.

The dynamic study carried out during the course of hot drawing shows evidence of relaxation processes of overstrains imposed on the amorphous chains in the necking stage. One may thus distinguish a transient orientation of the amorphous chains, which arises from the dynamics of crystal block rearrangement during necking, and a steady orientation enforced by the peculiar organization of the crystal blocks within the final fibrous structure. Strain-induced crystallization has also been shown to take place in the post-yield region through the orientational behaviour of the chain ends.

Although very useful for qualitative discussions, the comparison of the static and dynamic studies did not allow quantitative conclusions because of partial melting of the sample at the drawing temperature.

ACKNOWLEDGEMENTS

The authors wish to thank CdF Chimie SA for financial support of this work and a doctoral fellowship to J.D. The staff of the Application Laboratory of the CdF Chimie plant in Mazingarge are gratefully acknowledged for supplying the strips used in the dynamic study. We are also deeply indebted to M. Nicco of CdF Chimie and Professor Delhaye, Université de Lille, for their constant stimulation in the progress of this work.

REFERENCES

1 Siesler, H. W. and Holland-Moritz, K. 'Infrared and Raman Spectroscopy of Polymers', Marcel Dekker, New York, 1980
2 Koenig, J. L. *Adv. Polym. Sci.* 1983, **54**, 87
3 Siesler, H. W. *Adv. Polym. Sci.* 1984, **65**, 1
4 Seguela, R. and Rietsch, F. *Eur. Polym. J.* 1984, **20**, 765
5 Seguela, R. and Rietsch, F. *Polymer* 1986, **27**, 532
6 Seguela, R. and Rietsch, F. *Polymer* 1986, **27**, 703
7 Stein, R. S. and Norris, F. H. *J. Polym. Sci.* 1956, **21**, 381
8 Onogi, S. and Asada, T. *J. Polym. Sci., Polym. Symp.* 1967, **16**, 1445
9 Glenz, W. and Peterlin, A. *J. Macromol. Sci.–Phys. (B)* 1970, **4**, 473
10 Glenz, W. and Peterlin, A. *J. Polym. Sci., Polym. Phys. Edn.* 1971, **9**, 1191
11 Glenz, W. and Peterlin, A. *Makromol. Chem.* 1971, **150**, 163
12 McRae, M. A. and Maddams, W. F. *Makromol. Chem.* 1976, **177**, 473
13 McRae, M. A. and Maddams, W. F. *J. Appl. Polym. Sci.* 1978, **22**, 2761
14 Marikhin, V. A., Myashnikova, L. P., Novak, I. I., Suchkov, V. A. and Tukhvatullina, M. Sh. *Polym. Sci. USSR* 1972, **14**, 2865; *J. Polym. Sci., Polym. Symp.* 1972, **38**, 195
15 Holland-Moritz, K., Stach, W. and Holland-Moritz, I. *Prog. Colloid Polym. Sci.* 1980, **67**, 161
16 Holland-Moritz, K., Holland-Moritz, I. and Van Werden, K. *Colloid Polym. Sci.* 1981, **259**, 156
17 Siesler, H. W. *Infrared Phys.* 1984, **24**, 239
18 Steidl, J. and Pelzbauer, E. *J. Polym. Sci., Polym. Symp.* 1972, **38**, 345
19 Zachariades, A. E., Mead, W. T. and Porter, R. S. *Chem. Rev.* 1980, **80**, 351
20 Dupuis, J., Sombret, B., Legrand, P., Seguela, R. and Rietsch, F. *Polym. Bull.* 1987, **18**, 323
21 Krimm, S. *Adv. Polym. Sci.* 1960, **2**, 51
22 Snyder, R. G. *J. Chem. Phys.* 1967, **47**, 1316
23 Hoshino, S., Powers, J., Legrand, D. G., Kawai, H. and Stein, R. S. *J. Polym. Sci.* 1962, **58**, 185
24 Read, B. E. and Stein, R. S. *Macromolecules* 1968, **2**, 116
25 Suehiro, S., Yamada, T., Inagaki, H., Kyu, T., Nomura, S. and Kawai, H. *J. Polym. Sci., Polym. Phys. Edn.* 1979, **17**, 763
26 Kyu, T., Yamada, M., Suehiro, S. and Kawai, H. *Polym. J.* 1980, **12**, 809
27 Fujita, K., Suehiro, S., Nomura, S. and Kawai, H. *Polym. J.* 1982, **14**, 545
28 Hay, I. L. and Keller, A. *Colloid Polym. Sci.* 1965, **204**, 43
29 Peterlin, A. *Colloid Polym. Sci.* 1969, **233**, 857
30 Peterlin, A. and Meinel, G. *Makromol. Chem.* 1971, **142**, 227
31 Hosada, S. and Furuta, M. *Makromol. Chem. Rapid Commun.* 1981, **2**, 577
32 Hosada, S. *Makromol. Chem.* 1984, **185**, 787
33 Miller, P. J., Jackson, J. F. and Porter, R. S. *J. Polym. Sci., Polym. Phys. Edn.* 1973, **11**, 2001
34 Petracoone, V., Allegra, G. and Corradini, P. *J. Polym. Sci., Polym. Symp.* 1972, **38**, 419; *Macromolecules* 1971, **4**, 770
35 Oyama, T., Shiokawa, K. and Ishimaru, T. *J. Macromol. Sci.–Phys. (B)* 1973, **8**, 229
36 Painter, P. C., Havens, J., Hart, W. W. and Koenig, J. L. *J. Polym. Sci., Polym. Phys. Edn.* 1977, **15**, 1223
37 Predecki, P. and Statton, W. O. *J. Appl. Phys.* 1967, **38**, 4140; *J. Appl. Polym. Sci., Appl. Polym. Symp.* 1967, **6**, 165
38 Keith, H. D. and Passaglia, E. *J. Res. Nat. Bur. Stand. (A)* 1964, **68**, 513
39 Viovy, J. L., Monnerie, L. and Tassin, J.-F. *J. Polym. Sci., Polym. Phys. Edn.* 1983, **21**, 2427
40 Yoon, Do Y. and Flory, P. J. *Faraday Disc. Chem. Soc.* 1979, **68**, 288
41 Porter, R. S. and Johnson, J. F. *Chem. Rev.* 1966, **66**, 1
42 Hoffman, J. D., Guttman, C. M. and Di Marzio, E. A. *Faraday Disc. Chem. Soc.* 1979, **68**, 177